

See discussions, stats, and author profiles for this publication at: <https://www.researchgate.net/publication/234105225>

# Overriding the alkynophilicity of gold: catalytic pathways from higher energy Au(I)–substrate complexes and reactant deactivation via unproductive complexation in the gold(I)–catal...

ARTICLE *in* ORGANIC & BIOMOLECULAR CHEMISTRY · JANUARY 2013

Impact Factor: 3.56 · DOI: 10.1039/c2ob27231h · Source: PubMed

CITATIONS

10

READS

135

## 4 AUTHORS, INCLUDING:



**Dinesh V Vidhani**

Florida State University

11 PUBLICATIONS 95 CITATIONS

SEE PROFILE



**John Cran**

Florida State University

16 PUBLICATIONS 191 CITATIONS

SEE PROFILE



**Igor Alabugin**

Florida State University

142 PUBLICATIONS 3,549 CITATIONS

SEE PROFILE

# Organic & Biomolecular Chemistry

www.rsc.org/obc

Volume 11 | Number 10 | 14 March 2013 | Pages 1573–1744



ISSN 1477-0520

RSC Publishing

## PAPER

Marie E. Krafft, Igor V. Alabugin *et al.*

Overriding the alkynophilicity of gold: catalytic pathways from higher energy Au(I)–substrate complexes and reactant deactivation via unproductive complexation in the gold(I)-catalyzed propargyl Claisen rearrangement

# Overriding the alkynophilicity of gold: catalytic pathways from higher energy Au(I)–substrate complexes and reactant deactivation *via* unproductive complexation in the gold(I)-catalyzed propargyl Claisen rearrangement†

Dinesh V. Vidhani, John W. Cran, Marie E. Krafft\* and Igor V. Alabugin\*

Cite this: *Org. Biomol. Chem.*, 2013, **11**, 1624Received 20th October 2012,  
Accepted 23rd November 2012

DOI: 10.1039/c2ob27231h

www.rsc.org/obc

## Introduction

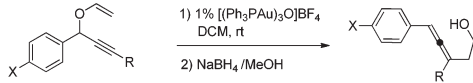
Gold-catalyzed cycloisomerizations and rearrangements of  $\pi$ -rich substrates find multiple applications in organic synthesis.<sup>1</sup> The common guiding principle in the design of Au-catalyzed organic reactions relies on the well-precedented “alkynophilicity” of gold.<sup>2</sup> Coordination at the triple bond increases alkyne electrophilicity and provides the rational foundation for the development of new Au-mediated reactions of alkynes. However, successful optimization of such catalytic processes in the presence of other functionalities relies on our knowledge of the low energy mechanistic pathways opened by catalyst/substrate interactions and on the understanding of how these pathways are influenced by the choice of reaction conditions and substituents.

Recently, Toste *et al.* reported an intriguing finding that both electron donors and electron acceptors at C4 (entries 1, 3 and 4, Table 1) slow down the Claisen rearrangement of propargylic vinyl ethers compared to the substrate with the unsubstituted phenyl ring (entry 2, Table 1).<sup>3</sup>

Considering the “alkynophilic” properties of Au(I), the above processes are expected to originate from the nucleophilic attack of the vinyl ether on the Au(I)-coordinated alkyne. However, in our experimental study of the allenyl vinyl ether

Computational and experimental analysis of unusual substituent effects in the Au-catalyzed propargyl Claisen rearrangement revealed new features important for the future development of Au(I) catalysis. Despite the higher stability of Au–alkyne complexes, they do not always correspond to the catalytically active compounds. Instead, the product emanates from the higher energy Au(I)–oxygen complex reacting *via* a low barrier cation-accelerated oxonia Claisen pathway. Additionally, both intra and intermolecular competition from other Lewis bases present in the system, for the Au(I) catalyst, can lead to unproductive stabilization of the substrate/catalyst complex, explaining hitherto unresolved substituent effects.

**Table 1** Experimental investigation of the gold(I)-catalyzed propargyl Claisen rearrangement performed by the Toste group

				
Entry	X	R	% Conv.	Time
1	OMe	$\eta^5$ -C <sub>4</sub> H <sub>9</sub>	89	12 h
2	H	CH <sub>2</sub> CH <sub>2</sub> OTBS	89	0.5 h
3	CF <sub>3</sub>	CH <sub>3</sub>	86	19 h
4	Br	<i>n</i> -C <sub>4</sub> H <sub>9</sub>	96	6.5 h

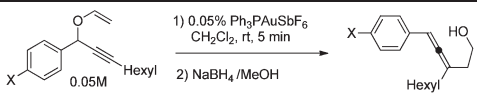
Claisen rearrangement, we observed products emanating from the coordination of Au(I) cations to the vinyl ether (VE) moiety in the presence of an allene moiety.<sup>4</sup> Considering the similarities between the allenyl vinyl ether rearrangement and the propargyl Claisen rearrangement reported by the Toste group, we undertook a mechanistic study into the nature of these Au-catalyzed processes.

## Results and discussion

Our experimental design kept substituents at the terminal alkyne atom constant while varying donor and acceptor groups at the carbinol carbon as in Toste's study. Despite the differences in the accelerating effects of the Ph<sub>3</sub>PAuSbF<sub>6</sub> and [(Ph<sub>3</sub>PAu)<sub>3</sub>O]BF<sub>4</sub> catalysts used in the two studies, we observed

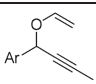
Department of Chemistry and Biochemistry, Florida State University, Tallahassee, FL 32306, USA. E-mail: mekrafft@fsu.edu, alabugin@chem.fsu.edu

†Electronic supplementary information (ESI) available. See DOI: 10.1039/c2ob27231h

**Table 2** Experimental substituent effects in the  $\text{Ph}_3\text{PAuSbF}_6$ -catalyzed propargyl Claisen rearrangement


Substrate	X	% Conv. <sup>a</sup>	Allene
1	OMe	21	7
2	Me	28	8
3	H	100	9
4	Cl	60	10
5	CF <sub>3</sub>	5	11
6	CN	Trace <sup>b</sup>	12

<sup>a</sup> Conversion in 5 minutes. <sup>b</sup> 100% conversion could only be achieved with 5% catalyst.

**Table 3** Computed activation and reaction energies (kcal mol<sup>-1</sup>) for the uncatalyzed Claisen rearrangement of aryl substituted propargyl vinyl ethers at the B3LYP/LANL2DZ and B3LYP/6-31G(d,p) levels


			$E_a$ (kcal mol <sup>-1</sup> ) (LANL2DZ)	$E_a$ (kcal mol <sup>-1</sup> )	NICS <sup>a</sup> (ppm)
15	Ph	TS1 <sup>H</sup>	22.3	23.4	-18.9
16	PhNH <sub>2</sub>	TS2 <sup>NH2</sup>	21.4	22.6	-17.6
17	PhNO <sub>2</sub>	TS3 <sup>NO2</sup>	22.0	23.4	-19.2

<sup>a</sup> B3LYP/6-31G(d,p) level.

the same unusual trend in which both electron donors and acceptors slowed down the reaction (Table 2).

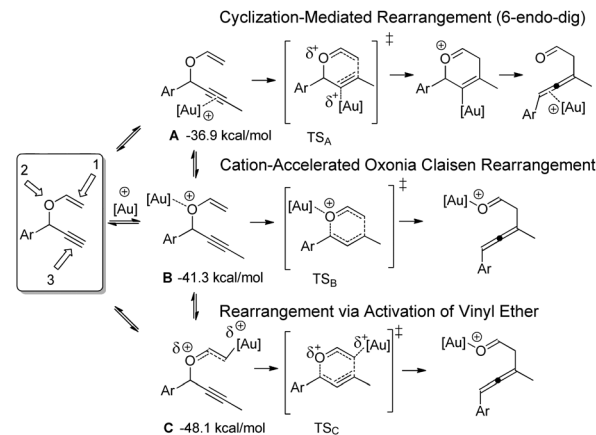
To understand the origin of this anomalous trend, we applied DFT calculations to the Au-catalyzed and uncatalyzed rearrangement of these substrates (see Computational methods). The uncatalyzed rearrangement was taken as the reference point. Comparison of B3LYP/LANL2DZ and B3LYP/6-31G(d,p) results for the non-catalyzed reaction (ESI<sup>†</sup>) found that the difference between the two basis sets is small and suggested that the B3LYP/LANL2DZ level is suitable for the further computational study.

The energies of the twist-boat and the twist-chair transition states are similar. Their geometries suggest concerted weakly asynchronous pathways similar to the uncatalyzed Claisen rearrangement of allyl vinyl ethers. The negative NICS values<sup>5</sup> in the geometric center of the forming rings confirm the aromatic nature of these transition states (Table 3).

Analysis of the Au-catalyzed reactions included three alternative mechanisms A–C based on the three Au-coordinating sites of the substrates<sup>6</sup> (Scheme 1). The computed complexation energies suggested an interesting coordinating preference: vinyl ether > oxygen > alkyne.<sup>7</sup>

#### A. Cyclization-mediated rearrangement and a “concealed” TS

The cyclization-mediated pathway<sup>8</sup> was originally considered for the  $[(\text{Ph}_3\text{Pau})_3\text{O}]\text{BF}_4$ -catalyzed propargyl Claisen<sup>3</sup> and propargyl ester<sup>9</sup> rearrangements by Toste and coworkers. The

**Scheme 1** Three mechanistic alternatives A–C for the Au(I)-catalyzed propargyl Claisen rearrangement and B3LYP/6-31G(d,p) binding energies for the three complexes.

process is sensitive to reaction conditions: the trapped cyclic products were absent when the reaction was performed in wet  $\text{CH}_2\text{Cl}_2$  but the formation of dihydropyran derivatives was observed in wet dioxane.<sup>10</sup> Our experiments with  $\text{Et}_3\text{PauCl}/\text{AgBF}_4$  also did not detect the trapped cyclic products in the presence of MeOH or *t*-BuOH in  $\text{CH}_2\text{Cl}_2$  (see ESI<sup>†</sup>).<sup>11</sup>

In concurrence with the earlier computational findings of the Toste group, we found only a single TS along this path and even an extensive IRC search could not locate a stationary point for the six-membered intermediate. The NICS and the HOMA<sup>12</sup> calculations for the three substrates showed moderately aromatic and asynchronous transition states (Table 4). Trends in the gas phase and solvent calculations were similar (Table 5).

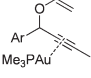
Several TS features are unusual and correspond to a stepwise process occurring *via* a six-membered intermediate instead of a concerted process. In particular, the C3–O4 bond cleavage ( $1.47 \rightarrow 1.54 \text{ \AA}$ ) (Fig. 1) was noticeably less pronounced in comparison to that in the uncatalyzed rearrangement ( $1.49 \rightarrow 2.03 \text{ \AA}$ ).<sup>13</sup>

The unusual reaction path, where the second “concealed” transition state<sup>14</sup> is buried in the PES continuum, combines the characteristics of a stepwise and a concerted pathway.<sup>15</sup> Although the IRC calculations did not locate the second transition state, the RMS gradient revealed the presence of a shallow inflection (Fig. 2) corresponding to the concealed transition state of the Grob-type fragmentation. Moreover, the NICS values showed the maximum aromaticity ( $-16.5 \text{ ppm}$ ) as the system progresses from the TS towards this inflection in a region where the calculated geometries are reminiscent of the cyclic intermediate and the 2nd TS.

The calculated geometries also reveal the source of selective stabilization for these “concealed” species: the Au cation changes its binding mode from a relatively weak  $\pi$ -coordination at the alkyne to the much tighter  $\sigma$ -bonding at the developing negative charge at C2 (the C2–Au distance change:  $2.245 \rightarrow 2.121 \text{ \AA}$ ).

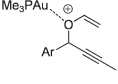


**Table 4** B3LYP/LANL2DZ activation and reaction energies for the gold(i)-catalyzed propargyl Claisen rearrangements

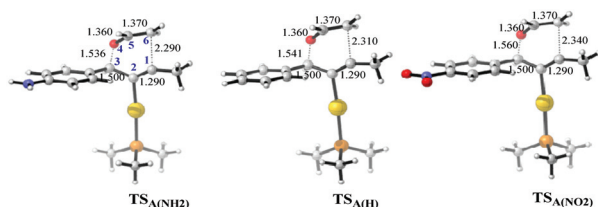
	$E_a^a$	$E_a^b$	$\Delta H^{\ddagger a}$	$\Delta G^{\ddagger a}$	$\Delta E_r^a$	NICS <sup>c</sup>	HOMA <sup>21</sup>
Ph	6.0 (7.3 <sup>d</sup> )	7.8	5.4	8.4	-26.7	-12.9	0.57
PhNH <sub>2</sub>	5.9 (7.1)	8.1	5.2	8.7	-33.9	-12.8	0.57
PhNO <sub>2</sub>	5.8 (6.8)	6.9	5.3	8.9	-24.3	-13.2	0.57

<sup>a</sup> B3LYP/LANL2DZ optimized geometries. <sup>b</sup> M05-2X optimized geometries. <sup>c</sup> GIAO/B3LYP/6-311+G(d,p). <sup>d</sup> Energies in parentheses include the solvation (CH<sub>2</sub>Cl<sub>2</sub>) correction.

**Table 5** Computed activation and reaction energies for the Au(i)-catalyzed cation-accelerated oxonia Claisen rearrangement of aryl substituted propargyl vinyl ethers at the B3LYP/LANL2DZ level

	$E_a^a$	$\Delta H^{\ddagger a}$	$\Delta G^{\ddagger a}$	$\Delta E_r^a$	NICS <sup>b</sup>	HOMA
Ar = PhNH <sub>2</sub>	4.9	3.7	5.8	-22.6	-12.6	0.23
Ar = PhOMe	6.8	6.1	5.0	-23.9	-14.0	0.52
Ar = Ph	8.8	7.3	8.9	-23.9	-15.6	0.74
Ar = PhCF <sub>3</sub>	8.4	6.9	9.7	-23.9	-15.6	0.75
Ar = PhCN	8.8	7.4	10.0	-25.3	-15.7	0.75
Ar = PhNO <sub>2</sub>	9.0	7.4	10.6	-26.2	-15.7	0.83

<sup>a</sup> Values calculated at the B3LYP/LANL2DZ level and expressed in kcal mol<sup>-1</sup>. <sup>b</sup> Values calculated at the GIAO/B3LYP/6-311+G(d,p) level.

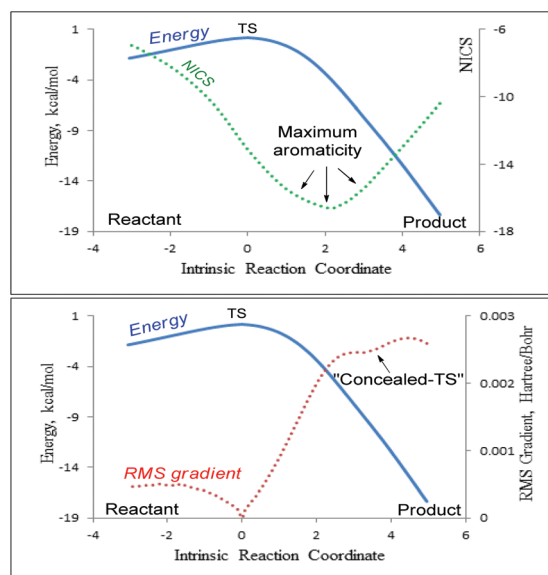
**Fig. 1** B3LYP/LANL2DZ TSs for the gold(i)-catalyzed cyclization-mediated Claisen-rearrangements of the three aryl-substituted propargyl vinyl ethers.

The absence of a discernible six-membered intermediate is consistent with our experimental findings whereas the important role of gold at this reaction stage suggests that slight modification in the nature of the catalyst (*e.g.*, the change from a mononuclear Au complex in our studies to the multi-nuclear Au catalyst used in the work of Toste) or solvent may indeed be sufficient for creating and trapping the cyclic intermediate.

Although the calculated effect of substituents was relatively small (Table 4 and Fig. 1 in ESI<sup>†</sup>), the trend indicated that, in contrast to the experimental substituent effects in Tables 1 and 2, donors should accelerate the reaction if it chooses to follow this path. Thus, we proceeded further down the list of possible mechanisms.

### B. Cation-accelerated oxonia Claisen rearrangement

Although cationic and anionic acceleration is well-documented for Claisen<sup>16</sup> and the oxy-Cope rearrangements,<sup>17</sup> this process

**Fig. 2** B3LYP/LANL2DZ IRC results for the gold(i)-coordinated substrate **15** (path A).

depends on coordination of Au(i), a soft Lewis acid, to oxygen instead of the polarizable  $\pi$ -bases. However, the calculated complexation energies suggest that coordination of the Au(i) catalyst to oxygen is favorable (*vide infra*). This observation is consistent with our experimental NMR ligand exchange studies where we observed the preferential coordination of Ph<sub>3</sub>PAuSbF<sub>6</sub> to the ethyl vinyl ether in the presence of 1-hexyne<sup>18</sup> and with the preferential coordination of Au(i) to the vinyl ether in the presence of alkyne observed in the gas-phase study of Roithová *et al.*<sup>7</sup>

Although most bond distances display moderate changes, the C3–O4 and C1–C6 bonds are much more elongated in the oxonia path than in the uncatalyzed and cyclization-mediated rearrangements (Fig. 3).

The IRC calculations showed a smooth potential energy surface indicative of a highly asynchronous but concerted pathway (Fig. 4).

Both energy and geometry of the highly polarized dissociative TS are profoundly influenced by the substituents (Table 5). In particular, the degree of asynchronicity is lower for the Ph, PhCF<sub>3</sub>, PhCN and PhNO<sub>2</sub> substituents (higher HOMA and NICS values, Table 5). The effect of the electron donating NH<sub>2</sub>

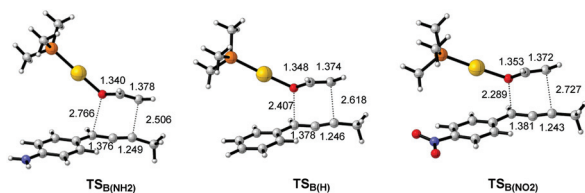


Fig. 3 B3LYP/LANL2DZ TSs for the Au(I)-catalyzed cation accelerated oxonia Claisen-rearrangements.

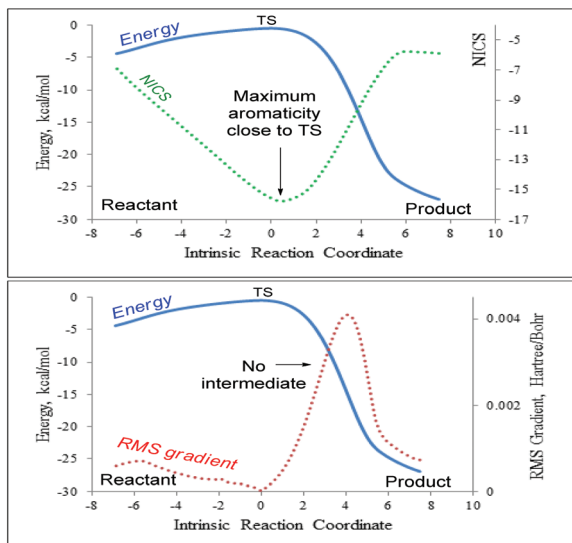


Fig. 4 B3LYP/LANL2DZ IRC calculations for the gold(I)-coordinated substrate 15 (path B).

group on the developing cationic center is even more pronounced than in path A and leads to a highly fragmented but noticeably stabilized TS.

Since our results for paths A and B could not explain the unusually slow reaction for the electron donating substituents, we considered the final mechanism *via* Au(I)-coordination at the vinyl ether  $\pi$ -system.

### C. Au(I)-coordination at the vinyl ether

The calculated transition states for this path display highly advanced C3–O4 bond cleavage with the concomitant cationic character accumulation at C3 which is even more pronounced than for the cation-accelerated oxonia Claisen rearrangement (Fig. 5).

As a result, a strong accelerating effect of the donating substituents is observed. Acceptors have a moderate decelerating influence. However, all calculated barriers remain significantly higher than for the previously discussed alternatives (Table 6). The calculated NICS values suggest that the electron donating substituents at the carbinol carbon stabilize the “fragmented-TS” while electron-withdrawing substituents force the TS to adopt a more symmetric geometry to avoid the build-up of positive charge on the carbinol carbon.

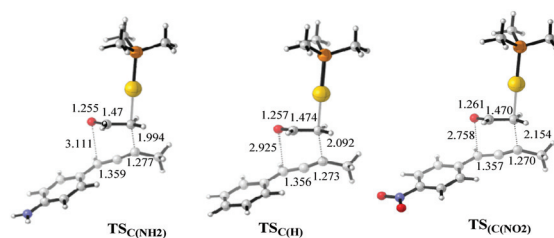


Fig. 5 B3LYP/LANL2DZ TSs for the gold(I)-catalyzed Claisen-rearrangements emanating from a Au(I)-VE complex.

Table 6 Computed activation and reaction energies for the Au(I)-catalyzed Claisen rearrangement of aryl substituted propargyl vinyl ethers emanating from a Au(I)-VE complex (B3LYP/LANL2DZ)

Ar	$E_a^a$	$\Delta H^\ddagger^a$	$\Delta G^\ddagger^a$	$\Delta E_r^a$	NICS <sup>b</sup>
Ar = PhNH <sub>2</sub>	25.1	23.7	25.0	−15.6	−8.1
Ar = PhOMe	26.5	24.7	26.2	−16.8	−8.8
Ar = Ph	28.7	26.9	27.8	−17.2	−9.9
Ar = PhCl	28.5	26.8	27.9	−17.6	−10.2
Ar = PhCN	29.2	27.4	28.5	−18.2	−10.9
Ar = PhNO <sub>2</sub>	29.8	28.5	27.7	−19.0	−11.7

All energies are in kcal mol<sup>−1</sup>. <sup>a</sup> Calculated at the B3LYP/LANL2DZ level. <sup>b</sup> Calculated at the GIAO/B3LYP/6-311+G(d,p) level.

### Curtin–Hammett analysis of the three pathways

The relative energies of the three transition states and products are presented in Fig. 6 relative to the energies of the isolated reactants. Although the Au(I)-coordinated vinyl ether complex has the lowest energy, the transition state energy is the highest among the three mechanisms. On the other hand, the cation-accelerated and the cyclization-mediated rearrangements are much closer in energies. The absolute TS energy is lower for the cation-accelerated Claisen rearrangement due to greater stability of the Au(I)-oxygen complex compared to the Au(I)-alkyne complex (Fig. 6).

The positive slope in the cation-accelerated rearrangement (slope = 2.8) and the rearrangement *via* Au(I)-coordinated vinyl ether (slope = 2.9) suggested build-up of a positive charge on the carbinol carbon while the slight negative slope for the cyclization mediated pathway (−1.0) indicated development of a negative charge on the carbinol carbon (Fig. 7).

Interestingly, the two low energy pathways converge at the electron withdrawing nitro substituent. A mechanistic shift towards a less-asynchronous pathway is predicted to occur in order to avoid the build-up of positive charge on the carbinol carbon.

Thus, the Curtin–Hammett analysis suggests a concerted cation-accelerated oxonia Claisen pathway *via* a “fragmented-TS” to be the most favorable among the three mechanisms. This pathway accounts for the failed attempts of trapping the six-membered intermediate. However, neither this path nor

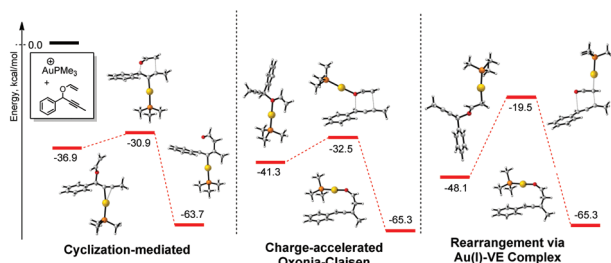


**Fig. 6** Curtin–Hammett analysis of the three mechanisms. Energies for the three pathways are given relative to the two non-interacting reagents.

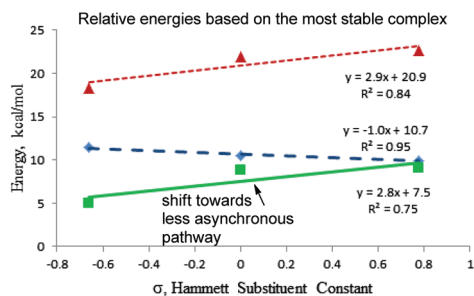


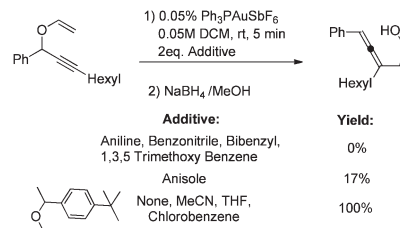
**Fig. 7** Correlation of Hammett substituent constants and the activation barrier for the three mechanisms (activation energies adjusted based on Curtin–Hammett correction). The red dashed line corresponds to the Au(I)–VE mechanism, the blue-dashed line corresponds to cyclization-mediated rearrangement and the solid green line represents cation-accelerated oxonia Claisen rearrangement.

the two higher energy alternatives can fully account for the experimentally observed substituent effects.

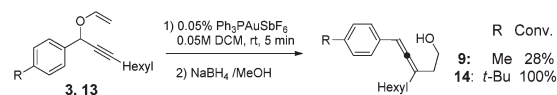
### Non-bonding interactions

In order to find a reason for the remaining discrepancy between the experimental and computational trends, we investigated the possibility of formation of Au-complexes with the “unproductive” Lewis bases present in the substrates. Our hypothesis was that the interaction of Au(I) with the lone-pairs of heteroatoms or the electron rich  $\pi$ -systems that do not take part in the reaction will influence the rate of the rearrangement. To test this hypothesis, we investigated the effect of additives on the rearrangement of vinyl ether **3** with an unsubstituted phenyl group on the carbinol carbon (Scheme 2).

For electron withdrawing substituents, the rate is affected by the electronic effect exerted by these groups on the rearrangement and by catalyst coordination at the heteroatoms. Both effects are decelerating. For the effect of electron donors, it may also include coordination at the aromatic  $\pi$ -systems. Indeed, when a sterically demanding *t*-Bu group was introduced at the aromatic moiety, the conversion improved from 28 to 100%. Clearly, this reactivity increase stems from the steric protection offered by the bulky substituent, preventing the unproductive cation– $\pi$  interaction with the Au(I)-catalyst (Scheme 3).



**Scheme 2** Effect of additives on the rearrangement.



**Scheme 3** Steric effect on the cation– $\pi$  interaction.

## Computational methods

All stationary point geometries in the uncatalyzed and gold(I) catalyzed Claisen rearrangements were optimized using the B3LYP functional<sup>19</sup> with the LANL2DZ basis set,<sup>20</sup> as implemented in the Gaussian03 package.<sup>21</sup> The effect of solvent (dichloromethane:  $\text{CH}_2\text{Cl}_2$ ) on the reaction barriers was evaluated using single point calculations with the PCM model at the SCRF-B3LYP/LANL2DZ level on the gas-phase geometries. Performance of the B3LYP method in studies of Au-catalyzed reactions has been tested extensively.<sup>22</sup> Frequency calculations confirmed that equilibrium geometries have all positive frequencies whereas transition state (TS) geometries had only one imaginary frequency (see ESI†). To test for the concerted nature of these reactions, the aromaticity of the selected TSs was examined using nucleus independent chemical shift (NICS(0))<sup>23</sup> and harmonic oscillator model of aromaticity (HOMA) methods. The nuclear independent chemical shift (NICS(0)) method introduced by Schleyer is one of the most commonly used, convenient and informative ways to study the aromaticity. It had been successfully applied to a variety of unusual structures, reactive intermediates and transition states and lent itself as a tool for better understanding of the allenic Claisen rearrangements.<sup>23</sup> The NICS(0) values for the Au(I)-containing species were calculated by the NMR-GIAO procedure at the B3LYP/LANL2DZ level. The B3LYP/6-311+G(d,p) level was used to compute NICS(0) values for non-catalyzed TSs. The HOMA, which is the geometry-based criteria of aromaticity, was calculated using the transition state geometry of the standard Claisen rearrangement of the allyl vinyl ether as a reference point (see ESI† for the detailed calculations). Intrinsic reaction coordinate (IRC) calculations were used to search for intermediates and additional transition states.

## Conclusions

In summary, the combination of experimental and computational studies of the Au-catalyzed propargyl Claisen

rearrangement provided us with new insights into the fundamental factors controlling the efficiency of Au(I) catalysis. Significantly, it was found that the product emanates from the higher energy Au(I)–oxygen complex, reacting *via* a low barrier cation-accelerated oxonia Claisen pathway, rather than *via* the more stable Au(I)–VE complex. Furthermore, calculations show that the “cyclization-mediated” pathway originating from the Au(I)–alkyne complex may be the kinetically competitive rearrangement mechanism as well.

From mapping the reaction potential energy surface with the nucleus independent chemical shift, a predicted 2nd TS for the cyclization-mediated pathway was found to be buried in the PES continuum. Stabilization of the 2nd TS and the related intermediate by coordination to the Au-catalyst explains why this TS, corresponding to the Grob-type fragmentation, is concealed and the “cyclization-mediated” process avoids the cyclization and follows instead an asynchronous concerted pathway.

Finally, the decelerating effect of electron donor groups was investigated through an experimental study of the effects of additives. The origin of this reaction deceleration, not predicted by a computational study, was revealed to be the result of unproductive coordination of Au(I) to either the electron rich  $\pi$ -systems or the heteroatomic Lewis bases which led to the stabilization of the starting materials.

These findings should help to shed light on other metal-mediated alkyne reactions and aid the development of new gold(I) catalyzed reactions.<sup>24</sup>

## Acknowledgements

Financial support by NSF (Grant CHE-1152491 to I. A. and CHE-0508969 to M. K.) and the MDS Research Foundation is gratefully acknowledged. We would also like to thank Dr Edwin F. Hilinski and Dr Manoharan Mariappan for their valuable suggestions.

## Notes and references

- 1 Z. Li, C. Brouwer and C. He, *Chem. Rev.*, 2008, **108**, 3239; N. Shapiro and F. D. Toste, *Synlett*, 2010, 675; A. S. K. Hashmi, *Angew. Chem., Int. Ed.*, 2010, **49**, 5232; A. Arcadi, *Chem. Rev.*, 2008, **108**, 3266; D. Benitez, N. D. Shapiro, E. Tkatchouk, Y. Wang, W. A. Goddard and F. D. Toste, *Nat. Chem.*, 2009, **1**, 482; A. Fürstner and P. W. Davies, *Angew. Chem., Int. Ed.*, 2007, **46**, 3410; K. Gilmore and I. V. Alabugin, *Chem. Rev.*, 2011, **111**, 6513; M. E. Krafft, D. V. Vidhani, J. W. Cran and M. Manoharan, *Chem. Commun.*, 2011, **47**, 6707; J. W. Cran and M. E. Krafft, *Angew. Chem., Int. Ed.*, 2012, **51**, 9398; R. J. Felix, D. Weber, O. Gutierrez, D. J. Tantillo and M. R. Gagné, *Nat. Chem.*, 2012, **4**, 405.
- 2 C. Nieto-Oberhuber, M. P. Munoz, E. Bunuel, C. Nevado, D. J. Cardenas and A. M. Echavarren, *Angew. Chem., Int. Ed.*, 2004, **43**, 2402; L. Zhang, J. Sun and S. A. Kozmin, *Adv. Synth. Catal.*, 2006, **348**, 2271.
- 3 B. D. Sherry and F. D. Toste, *J. Am. Chem. Soc.*, 2004, **126**, 15978.
- 4 Original report: M. E. Krafft, K. M. Hallal, D. V. Vidhani and J. W. Cran, *Org. Biomol. Chem.*, 2011, **9**, 7535.
- 5 (a) K. N. Houk, J. Gonzalez and Y. Li, *Acc. Chem. Res.*, 1995, **28**, 81; (b) K. N. Houk, Y. Li and J. D. Evanseck, *Angew. Chem., Int. Ed. Engl.*, 1992, **31**, 682; (c) M. J. S. Dewar and C. Jie, *Acc. Chem. Res.*, 1992, **25**, 537; (d) H. Jiao and P. v. R. Schleyer, *J. Phys. Org. Chem.*, 1998, **11**, 655.
- 6 Because the experimental performance of  $\text{Ph}_3\text{PAuSbF}_6$  and  $\text{Et}_3\text{PAuSbF}_6$  is similar, we chose  $\text{Me}_3\text{PAu(I)}$  as the model Au(I) species to maximize the computational efficiency.
- 7 Gas phase experimental  $\text{Me}_3\text{PAu}^+$  binding trends display a similar trend: methyl vinyl ether > acetylene. (a) J. Roithová, J. Hrušák, D. Schröder and H. Schwarz, *Inorg. Chim. Acta*, 2005, **358**, 4287; (b) J. Roithová, Š. Janková, L. Jašíková, J. Váňa and S. Hybelbauerová, *Angew. Chem., Int. Ed.*, 2012, **124**, 8503; (c) L. Jašíková and J. Roithová, *Organometallics*, 2012, **31**, 1935.
- 8 The cyclization mediated pathway was first proposed by the Overman group for Pd(II) and Hg(II)-catalyzed [3,3] sigma-tropic rearrangements. L. E. Overman, *Angew. Chem., Int. Ed. Engl.*, 1984, **23**, 579.
- 9 P. Mauleon, J. L. Krinsky and F. D. Toste, *J. Am. Chem. Soc.*, 2009, **131**, 4513.
- 10 B. D. Sherry, L. Maus, B. N. Laforteza and D. Toste, *J. Am. Chem. Soc.*, 2006, **128**, 8132.
- 11 The reaction was extremely fast compared to the phenyl analogs. Thus, the  $\text{BF}_4$  counter-ion, which showed a slower reaction compared to the  $\text{SbF}_6$  counter-ion, was used for this study.
- 12 J. Kruszewski and T. M. Krygowski, *Tetrahedron Lett.*, 1972, **36**, 3839; T. M. Krygowski, *J. Chem. Inf. Comput. Sci.*, 1993, **33**, 70; B. T. Stępień, T. M. Krygowski, M. K. Cyrański, J. Młochowski, P. Orioli and F. Abbate, *ARKIVOC*, 2004, 185. The HOMA is calculated using  $\text{rHOMA} = 1 - \alpha/n\Sigma(R_0 - R_i)^2$ ,  $\alpha = 2\{(R_0 - R_S)^2 - (R_0 - R_D)^2\}^{-1}$ . The allyl vinyl ethers are known to rearrange *via* an aromatic transition state. Thus, for our case,  $R_0$  values were used as the reference point for calculating the transition state geometries of the thermal Claisen rearrangement of allyl vinyl ether. The  $\alpha$ -value for each bond was calculated separately.
- 13 Not only is the C–O bond not broken in the rate-limiting step but the other bonds showed relatively small changes relative to the reactant (C1–C2: 1.25  $\rightarrow$  1.29 Å; C2–C3: 1.51  $\rightarrow$  1.50 Å; O4–C5: 1.41  $\rightarrow$  1.36 Å; C5–C6: 1.34  $\rightarrow$  1.37 Å).
- 14 (a) H. Joo, E. Kraka, W. Quapp and D. Cremer, *Mol. Phys.*, 2007, **105**, 2697; (b) D. V. Vidhani, J. W. Cran, M. E. Krafft, M. Manoharan and I. V. Alabugin, *J. Org. Chem.*, 2012, **77**, DOI: 10.1021/jo302152j.
- 15 (a) W. R. Roth, D. Wollweber, R. Offerhas, V. Rekowski, H. W. Lennartz, R. Sustmann and W. Müller, *Chem. Ber.*, 1993, **126**, 2701; (b) D. A. Hrovat, J. A. Duncan and W. T. Borden, *J. Am. Chem. Soc.*, 1999, **121**, 169;



- (c) P. Caramella, P. Quadrelli and L. Toma, *J. Am. Chem. Soc.*, 2002, **124**, 1130; (d) D. J. Tantillo, *J. Phys. Org. Chem.*, 2008, **21**, 561; (e) D. H. Nouri and D. J. Tantillo, *J. Org. Chem.*, 2006, **71**, 3686; (f) Aromatic TS for a non-pericyclic reaction: K. Gilmore, M. Manoharan, J. Wu, P. v. R. Schleyer and I. V. Alabugin, *J. Am. Chem. Soc.*, 2012, **134**, 10584.
- 16 (a) K. Takai, I. Mori, K. Oshima and H. Nozaki, *Tetrahedron Lett.*, 1981, **22**, 3985; (b) K. Takai, I. Mori, K. Oshima and H. Nozaki, *Bull. Chem. Soc. Jpn.*, 1984, **57**, 446; (c) J. W. S. Stevenson and T. A. Bryson, *Tetrahedron Lett.*, 1982, **23**, 3143; (d) K. Takai, I. Mori, K. Oshima and H. Nozaki, *Tetrahedron*, 1984, **40**, 4013; (e) K. Maruoka, S. Saito and H. Yamamoto, *J. Am. Chem. Soc.*, 1995, **117**, 1165.
- 17 (a) D. A. Evans and A. M. Golob, *J. Am. Chem. Soc.*, 1975, **97**, 4765; (b) B. K. Carpenter, *Tetrahedron*, 1978, **34**, 1877; (c) D. A. Evans, D. J. Ballalargeon and J. V. Nelson, *J. Am. Chem. Soc.*, 1978, **100**, 2242; (d) R. Pal, R. J. Clark, M. Manoharan and I. V. Alabugin, *J. Org. Chem.*, 2010, **75**, 8689.
- 18 Monitoring of NMR spectra of the 1:1 mixture of ethyl vinyl ether and 1-hexyne with 1 equivalent of  $\text{Ph}_3\text{PAuSbF}_6$  in  $\text{CD}_2\text{Cl}_2$  revealed that vinyl ether protons completely disappear while alkyne protons were still present. See ESI† for the additional details.
- 19 A. D. Becke, *J. Chem. Phys.*, 1993, **98**, 5648; A. D. Becke, *Phys. Rev. A*, 1998, **38**, 3098; C. Lee, W. Yang and R. G. Paar, *Phys. Rev. B: Condens. Matter*, 1980, **37**, 785.
- 20 (a) T. H. Dunning and P. J. Hay, in *Methods of Electronic Structure Theory*, ed. H. F. Schaefer III, Plenum, New York, 1976, vol. 2 and 3, pp. 1–28; (b) P. J. Hay and W. R. Wadt, *J. Chem. Phys.*, 1985, **82**, 270; (c) P. J. Hay and W. R. Wadt, *J. Chem. Phys.*, 1985, **82**, 284; (d) P. J. Hay and W. R. Wadt, *J. Chem. Phys.*, 1985, **82**, 299; (e) C. E. Check, T. O. Faust, J. M. Bailey, B. J. Wright, T. M. Gilbert and L. S. Sunderlin, *J. Phys. Chem. A*, 2001, **105**, 8111.
- 21 See ESI† for the complete reference. M. J. Frisch, *et al.*, *GAUSSIAN 03 (Revision E.01)*, Gaussian, Wallingford, CT, 2004.
- 22 (a) G. Lemiere, V. Gandon, K. Cariou, A. Hours, T. Fukuyama, A.-L. Dhiman, L. Fensterbank and M. Malacria, *J. Am. Chem. Soc.*, 2009, **131**, 2993; (b) J.-M. Tang, S. Bhunia, S. Md. A. Sohel, M.-Y. Lin, H.-Y. Liao, S. Datta, A. Das and R.-S. Liu, *J. Am. Chem. Soc.*, 2007, **129**, 15677; (c) Y. Xia, A. S. Dudnik, V. Gevorgyan and Y. Li, *J. Am. Chem. Soc.*, 2008, **130**, 6940; (d) G. Kovacs, G. Ujaque and A. Lledos, *J. Am. Chem. Soc.*, 2008, **130**, 853; (e) I. Alonso, B. Trillo, F. Lopez, S. Montserrat, G. Ujaque, L. Castedo, A. Lledos and J. L. Mascarenas, *J. Am. Chem. Soc.*, 2009, **131**, 13020; (f) P. H.-Y. Cheong, P. Morganelli, M. R. Luzung, K. N. Houk and F. D. Toste, *J. Am. Chem. Soc.*, 2008, **130**, 4517.
- 23 (a) H. Jiao and P. v. R. Schleyer, *Angew. Chem., Int. Ed. Engl.*, 1993, **32**, 1763; (b) R. Herges, H. Jiao and P. v. R. Schleyer, *Angew. Chem., Int. Ed. Engl.*, 1994, **33**, 1376; (c) H. Jiao and P. v. R. Schleyer, *J. Chem. Soc., Perkin Trans. 2*, 1994, 407; (d) H. Jiao and P. v. R. Schleyer, *J. Chem. Soc., Faraday Trans.*, 1994, **90**, 1559; (e) H. Jiao and P. v. R. Schleyer, *J. Am. Chem. Soc.*, 1995, **117**, 11529; (f) H. Jiao and P. v. R. Schleyer, *Angew. Chem., Int. Ed. Engl.*, 1994, **34**, 334.
- 24 See for example: (a) S. Naoe, Y. Suzuki, K. Hirano, Y. Inaba, S. Oishi, N. Fujii and H. Ohno, *J. Org. Chem.*, 2012, **77**, 4907; (b) A. S. K. Hashmi, I. Braun, M. Rudolph and F. Rominger, *Organometallics*, 2012, **31**, 644; (c) P. M. Byers, J. I. Rashid, R. K. Mohamed and I. V. Alabugin, *Org. Lett.*, 2012, **14**, 6032.